

THE USE OF A FREQUENCY DOMAIN STEPPED FREQUENCY TECHNIQUE TO OBTAIN HIGH RANGE RESOLUTION ON THE CSIR X-BAND SAR SYSTEM

Willie Nel, CSIR Defencetek, Pretoria, South Africa
Jan Tait, CSIR Defencetek, Pretoria, South Africa
Richard Lord, University of Cape Town, South Africa
Andrew Wilkinson, University of Cape Town, South Africa

1 ABSTRACT

A novel Frequency Domain, Stepped Frequency Processing (FD-SFP) technique to obtain high radar range resolution was developed by AJ Wilkinson in 1997. Range resolution is directly related to the measurement bandwidth of a radar system. The FD-SFP technique pieces together several sub portions of the target scene reflectivity spectrum to form a high resolution radar range return. This paper demonstrates the use of the FD-SFP algorithm on the CSIR X-Band experimental SAR system (RoofSAR). Some issues arising in practical implementation of the technique are discussed. Results of using the technique on radar data recorded by the RoofSAR are presented. It is concluded that the technique provides a viable option for generating SAR imagery with high range resolution and an acceptable level of ghosting artifacts.

2 INTRODUCTION

Synthetic Aperture Radar (SAR), initially developed in 1951 by C Wiley, is a well-known imaging radar technique that aims to produce high resolution images of an area of interest. Originally, the aim of SAR was to improve the radar sensor azimuth resolution to be comparable to the range resolution. Over time the SAR azimuth processing techniques have improved to such an extent, that the limits of SAR image resolution in the range dimension have again become an issue for modern-day digital SAR systems.

The laws of physics dictate that the maximum obtainable range resolution is inversely proportional to the bandwidth over which a target scene's reflectivity spectrum is observed¹. The maximum obtainable radar range resolution $\delta_{R_{max}}$, given an observation of a scene over a bandwidth B , can be expressed as

$$\delta_{R_{max}} = \frac{c}{2B} \quad (1)$$

¹In this context *resolution* is a measurement of the ability of the radar to discern spatially close targets.

where c is the propagation speed of electromagnetic radiation.

Current high resolution SAR imaging systems aim to produce SAR imagery at resolutions less than 10 cm. From Eq. 1, it can be seen that obtaining such high range resolution requires measurement bandwidths wider than 1 GHz. Achieving these types of bandwidths directly as the instantaneous bandwidth of the radar is very costly². Therefore, other techniques to attain this bandwidth have to be considered.

The CSIR X-Band experimental SAR system (known as the RoofSAR [2]) aims to produce SAR images at resolutions lower than 30 cm. To achieve the required wide measurement bandwidth, the system employs a stepped frequency transmitter/receiver system, together with a *Frequency Domain Stepped Frequency Processing* (FD-SFP) technique for reconstruction of the wide bandwidth scene reflectivity spectrum.

In SFP techniques [1, 3], the transmit bandwidth is broken into smaller sub-bands and radar range data is recorded separately for the different bands. The data is then combined, to reconstruct a larger portion of the scene reflectivity spectrum. If not designed properly, SFP techniques can produce high resolution range lines that contain artifacts known as ghosting artifacts. These artifacts are undesirable when producing SAR images.

The FD-SFP technique implemented for the RoofSAR system [4] was designed to reduce these undesired artifacts. The original work tested the developed algorithm on simulated data over a 100 MHz bandwidth. The current paper aims to extend this work by investigating issues around the practical implementation of this FD-SFP technique for use over bandwidths of more than 1 GHz.

²Due to the high cost of high speed A/D devices and the difficulty of designing custom digital recording equipment that can record data at these rates.

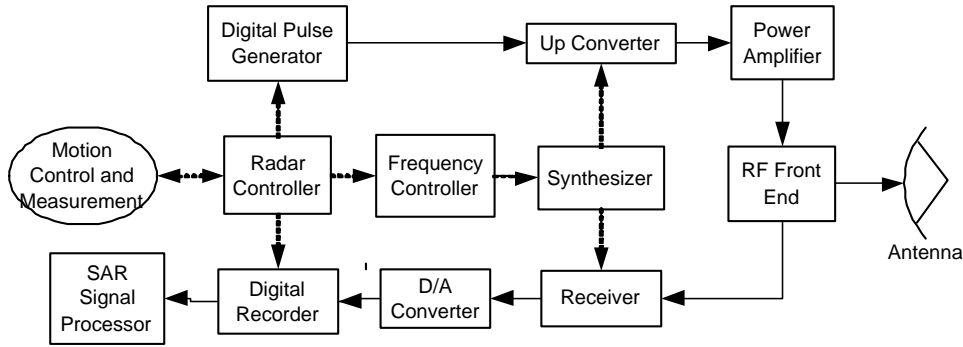


Figure 1: RoofSAR System Block Diagram



Figure 2: The RoofSAR system

3 SYSTEM DESCRIPTION

Figure 1 shows a block diagram of the radar system³. The system is mounted on a rail on the roof of a building at the CSIR (see Figure 2). Platform motion is controlled and measured by the Motion Control Unit (MCU). At specified intervals on the rail, the MCU triggers the radar controller to generate a burst of radar pulses, each pulse at a different centre frequency, as controlled by the frequency controller⁴. The transmit pulse is generated by a programmable D/A converter. At each frequency in the burst, radar range return data is sampled (8-bit) at IF ⁵ and stored at a rate of 80 MS/sec by the digital recorder.

The SAR signal processor takes this raw radar data (still at IF) as an input, and converts it to quadrature baseband signals using a digital quadrature demodulation technique⁶. After this, pulse compression is performed to produce the raw baseband radar range returns. Next, the range lines from a burst of frequencies is combined into a single range line using the FD-

³A more detailed system description is presented in [2].

⁴The radar has an agile bandwidth of 1.2 GHz.

⁵The IF frequency is 20 MHz.

⁶Digital I/Q demodulation techniques are more stable than analog techniques since they do not suffer from temperature and path length effects.

SFP technique described in the next section. Lastly, azimuth compression is performed, and a SAR image is produced. Note that the system does not employ a motion compensation stage, since the motion control and measurement unit automatically ensures even samples in the along track dimension (and the rail ensures stability in the range dimension).

When recording a set of RoofSAR data, the system generates an enormous amount of data. Typically, data is sampled at a 5 cm interval over the 130m rail, with 161 frequency steps per burst, and 2048 samples per range line at 1 byte per sample. This results in a raw data file size of approximately 820MB. After this, the data is I/Q demodulated and pulse compression performed, the data size for this set-up actually increases to around 3 GB, since the pulse compression processing generates a 4 byte floating point output. Thus, the efficiency of the FD-SFP algorithm to handle large amounts of data and still process it in a reasonable time is also important.

4 THE FD-SFP ALGORITHM

The FD-SFP algorithm is completely described in [4]. The important aspects of the original algorithm is summarised here for ease of reference.

1. Choose a set of n radar centre frequencies f_1, f_2, \dots, f_n separated by Δf such that Δf is marginally less than the radar instantaneous bandwidth B_{tx} . If $\Delta f > B_{tx}$, the resulting measurements will contain gaps in the reflectivity spectrum, possibly yielding ghosting artifacts.
2. At each centre frequency, obtain a sampled version of the coarse resolution radar range line $v_{bb_{f_1}}(t), \dots, v_{bb_{f_n}}(t)$ starting at $t = t_0$. The range lines are sampled at a complex sample rate $f_s \geq B_{tx}$.
3. Convert each range line to the frequency domain yielding a set of frequency domain data

$$V_{bb_{f_1}}(f), \dots, V_{bb_{f_n}}(f).$$

4. Shift the spectrum of range line i to the appropriate location centred on $f_i = (i + \frac{1-n}{2})\Delta f$.
5. Form a combined spectrum $V_{comb}(f)$ of the n range lines by coherently adding or splicing the different sub-spectra together.
6. Multiply the combined spectrum by an appropriate compression filter $H(f)$. $H(f)$ has the function of correcting for phase and amplitude errors/irregularities in the system response.
7. Apply a window (such as a hamming or hanning window) to the combined spectrum if required.
8. Finally, generate the time domain high resolution range line using an inverse Fourier transform.

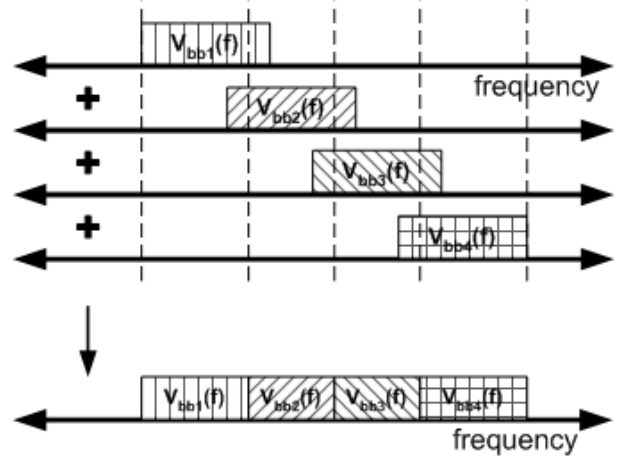


Figure 3: Splicing together 4 different baseband sub-spectra.

5 IMPLEMENTATION OF THE ALGORITHM

To obtain an efficient implementation of the FD-SFP algorithm, some careful choices of the parameters could be made to simplify the amount of processing involved.

The required frequency shift in Step 4 of the algorithm can be achieved by multiplying with a linear phase ramp in the time domain or by using a cut and paste method in the frequency domain. The cut and paste method results in a much more efficient algorithm, but can only be used if the number of frequency bins by which the sub spectrum is shifted, is an integer multiple of the frequency interval Δf_{DFT} represented by each bin of the spectrum in the frequency domain.

Given that some discrete implementation of the Fourier transform is used in Step 3 to produce this sub spectrum, this frequency interval Δf_{DFT} is calculated as

$$\Delta f_{DFT} = \frac{f_s}{n_{bins}} \quad (2)$$

where n_{bins} equals the number of bins over which the DFT is performed.

The number of bins n_{shift} by which adjacent steps are to be moved in frequency, is given by

$$n_{shift} = \frac{\Delta f}{\Delta f_{DFT}} \quad (3)$$

The final algorithm was designed for a choice of system parameters such that n_{shift} is an integer. The process of pasting together the different sub-spectra is illustrated in Figure 3 for the combination of 4 sub-spectra. For each measurement, the valid portion of the sub spectrum is found and copied to a new array at the correct centre frequency⁷. Since the algorithm re-

⁷Note that the lowest and highest sub-spectra adds slightly wider frequency sections to the final spectrum.

quires large amounts of data to be converted from the frequency to the time domain and back, the choice of fast Fourier algorithm was important. Some FFT algorithms require the input vector length to be an integer power of 2. In Step 8, this can sometimes result in a large zero padding exercise since, for example, you could end up with the number of samples equalling 9000, in which case the next power of 2 would be 16384. To avoid zero padding issues, it was decided to use an algorithm that can perform fast Fourier transforms on range lines of any number of samples. The algorithm entitled "the Fastest Fourier Transform in the West" (FFTW [5]) is a very fast and efficient algorithm that is widely used. Some benchmarks indicating that the FFTW algorithm performs very well on longer (>1024 samples) 1D FFT's when compared to other available FFT algorithms, are available.

The final implementation was coded in C using the FFTW algorithm and a cut and paste method for the frequency reconstruction.

6 EXPERIMENTAL SETUP

Apart from issues related to speed, some issues relating to the overall performance of the FD-SFP algorithm were also identified during development and testing.

6.1 CHOOSING THE TRANSMIT BANDWIDTH AND STEPSIZE

A possible cause of ghosting artifacts in the resulting high resolution range line, was due to phase non-linearity effects at the boundaries of adjacent frequency steps. According to the properties of the Fourier transform, any periodic amplitude and phase discontinuity in the spectrum could cause a resulting pulse train in

the time domain. These pulse trains show up as ghosting artifacts or sidelobes in the reconstructed range line.

Although the reconstruction filter $H(f)$ is used to cancel these effects, any instability or change in the phase of the instantaneous system phase response could result in the increase of these ghosting artifacts. Since, at the filter edges, the transfer function of the filters are most sensitive to phase changes with changes in system temperature, care was taken in choosing the final transmitted pulse bandwidth B_{tx} not to include these frequencies in the transmit signal. For this reason, the final bandwidth used for the experiments was only 75% of the actual system instantaneous bandwidth.

6.2 IMPORTANCE OF THE CORRECTION FILTER

Special mention should also be made of the construction of the correction filter $H(f)$. Since $H(f)$ should include all system effects, it should be constructed using actual measured data of a point target reflector so that all possible sources of error in the radar transmitter and receiver are included in the filter. If this is not done, the final phase error in the system could still contain periodic energy that will result in ghosting artifacts in the time domain.

This philosophy was verified with the RoofSAR system, since even the calibration filter constructed by using a RF front end calibration path to couple transmit energy into the receiver produced results that still contain significant artifacts. These artifacts were caused by a few components of the system (such as the T/R switch), that were not included in this correction.

In the final experiments $H(f)$ was obtained by passing point target data obtained from measurements of a corner reflector (mounted on a mast covered in radar absorptive material) through the exact same processing as the normal radar data.

Blindly using the correction filter $H(f)$ obtained in this way resulted in a range shift of the final high resolution range line, such that the corner reflector return was positioned in range bin 1. This happened, since the zero phase point of the radar after correction with $H(f)$ was located at the position of the corner reflector.

To correct the phase of the final data so that no range shift is introduced, the range bin containing the peak of the uncalibrated point target return after applying FD-SFP (but without applying $H(f)$) were estimated from the data. This range was then be used to calculate a correction phase ramp by which to multiply $H(f)$ such that calibrated range lines had the correct range delay/position. Also note that a shift in range causes defocussing during the azimuth compression stage, which requires an accurate value for the time delay to the first range bin.

6.3 EXPERIMENTAL SETUP

The final radar setup used to generate the results presented here is shown in Table 1.

Table 1: Radar Setup used to generate results

Parameter	Value
Δf	7.5 MHz
Chirp Bandwidth (B_{tx})	15 MHz
Steps used	161
n_{bins} after I/Q demodulation	200
Radar Centre Frequency	X - Band

The first target used during the experiments was a trihedral corner reflector mounted on a mast, such that the corner reflector was lifted above most of the ground clutter in the region. The mast was covered with radio-frequency absorber material with an approximate two-way absorption of 40 dB at X-Band.

The second set of data was captured by the RoofSAR to form a SAR image of the area below the building where the rail was mounted. Two targets, a 4x4 vehicle and a tank were parked in the area.

7 RESULTS

In Figure 7(a) the coarse resolution radar return $v_{bb_{f_1}}(t)$ from the corner reflector at the first transmit frequency is shown.

(b) shows the amplitude of the spectrum $V_{comb}(f)$ of the combined steps *without* applying any system calibration. The frequency response as illustrated in (b) is inverted ($\frac{1}{\sqrt{V_{comb}(f)}}$) to obtain the correction filter $H(f)$. (c) shows the point target response (time domain) of the system without performing any calibration.

In (d) the process is now repeated on the next burst of data that was recorded during the same data set, this time using $H(f)$ as the correction filter for removing system induced artifacts in the range returns of the data. Since the data was recorded within milliseconds of each other, it is seen that the system shows very good results in terms of suppressing the ghosting artifacts that were present in (c).

(e) was produced to validate the process further. Here $H(f)$ was applied to a second data take at a different time. In this case it is seen that the correction filter has decorrelated somewhat, and the ghosting artifacts are much more pronounced again. However, the peak sidelobe (ghosting) level is decreased by almost 18 dB when compared to (c) from -5 dB to -23 dB.

(h) shows the final SAR image obtained by the system. The tank is seen as the very bright feature at a range of about 75 m. In (g) it is seen that the image obtained without applying the correction filter contains

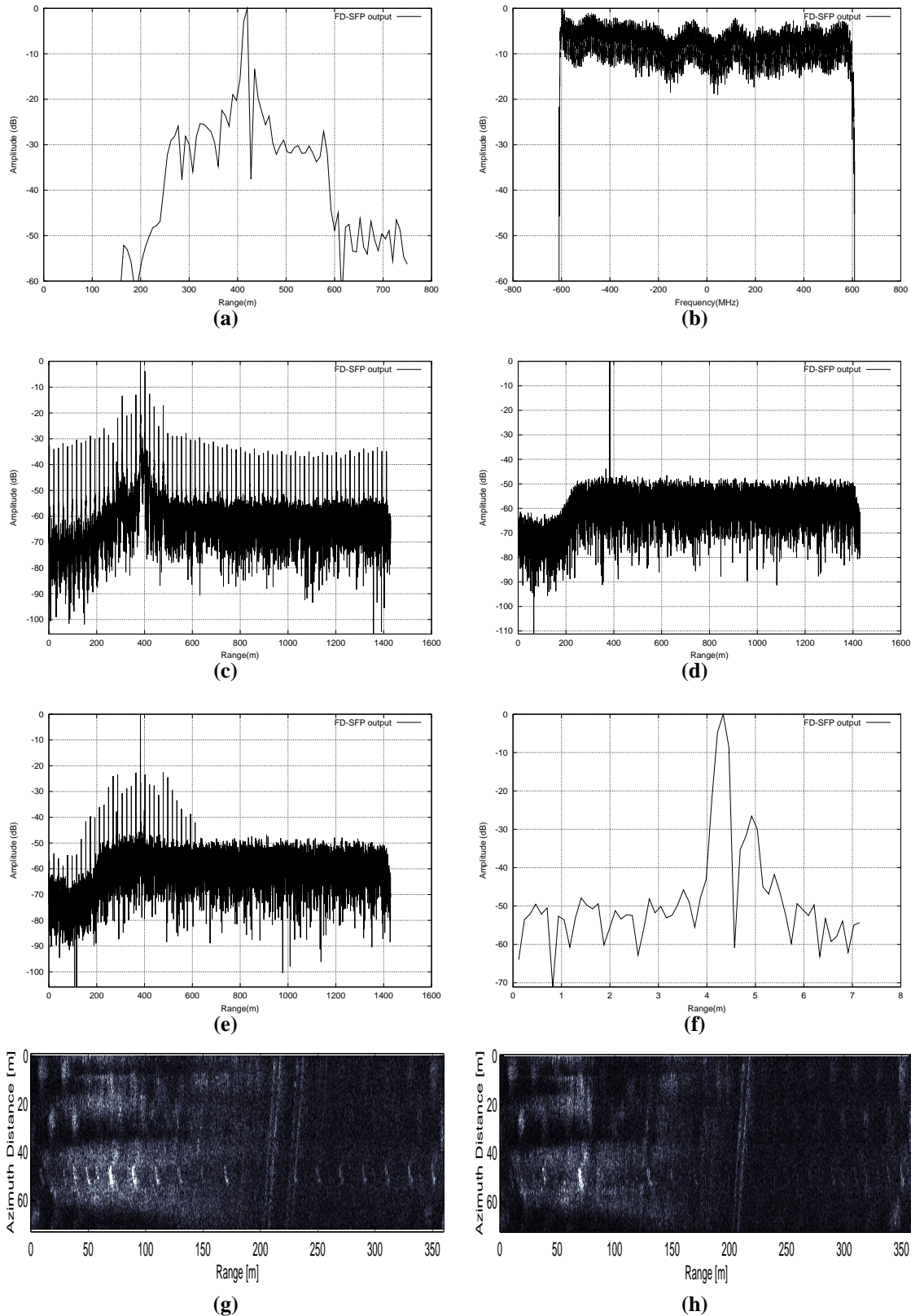


Figure 4: Results. **(a)** Coarse resolution, range compressed radar return from calibration target. **(b)** Frequency response after adding different sub-spectra without applying $H(f)$. **(c)** Point target response without applying $H(f)$ for correction. **(d)** Point Target Response by applying $H(f)$ to next burst of data in the same data take. **(e)** Point Target Response by applying $H(f)$ to data from a different data take. **(f)** Zoomed version of **(e)** to show resolution of point target. **(g)** Image obtained without using $H(f)$ for calibration. **(h)** SAR image obtained by using $H(f)$ for calibration. The image in **(g)** contains more pronounced ghosting effects than the image in **(h)**.

many ghosting artifacts which cause multiple images of the tank (and other objects) to appear in the image. For a detailed description of this image see [2].

Comparing the 3 dB resolution of the peak in (a) with that of (f), it is clearly seen that the FD-SFP technique has increased the resolution from about 10m in the coarse range data to better than 20cm in the output.

The final implemented FD-SFP code executed quite quickly, taking approximately 5 seconds to perform the processing for 1031 bursts of data (about 1.2 GBytes) on a 1.1 GHz Athlon processor with 256MB RAM.

8 CONCLUSION

Stepped frequency processing techniques enable the generation of high range resolution radar returns without the cost of very high instantaneous bandwidth. The FD-FSP algorithm presented proves to be a successful technique to perform such stepped frequency processing, even if the total amount of bandwidth considered is very large. The implemented algorithm significantly suppressed unwanted ghosting artifacts. This ability is largely due to the use of a good calibration process, and illustrates the importance of such a calibration procedure for radars using SFP techniques to process their data. The algorithm also proved to be fast enough for use on practical (large) data sets.

However, it was observed that long term drifting effects in the radar system still caused significant ghosting artifacts due to decorrelation of the calibration filter. Future work could include investigations into ways of obtaining calibration data that is less prone to decorrelation. This could be done by using an RF front-end calibration path to record data every time the system is used, and then augmenting this data with a single measurement of the sub-systems not included in this calibration path (such as the Antenna and T/R switch).

9 ACKNOWLEDGEMENTS

The authors would like to thank everyone at the CSIR and UCT involved in the RooFSAR project. Funding for this project was provided by Armscor.

REFERENCES

- [1] W. G. Carrara, R. S. Goodman, and R. M. Mawjowski, *Spotlight Synthetic Aperture Radar: Signal Processing Algorithms*. Boston, London: Artech House, first ed., 1995.
- [2] J. Tait and W. Nel, "X-band synthetic aperture radar evaluation platform," *IEEE Africon 2002*, October 2002.

- [3] D. Wehner, *High Resolution Radar*. 685, Canton Street, Norwood: Artech House, first ed., 1987.

- [4] A. J. Wilkinson, R. T. Lord, and M. R. Inggs, "Stepped-frequency processing by reconstruction of target reflectivity spectrum," *Proceeding of the 1998 IEEE South African Symposium on Communications and Signal Processing (COMSIG '98)*, pp. 101–104, September 1998.

- [5] M. Frigo and S. Johnson, "The fastest fourier transform in the west," *Technical Report, MIT*, September 1997.

Principal Author: W. A. J. Nel received a B.Eng (Electronic) degree from the University of Pretoria, South Africa, in 1996. He completed his M.Sc(Eng) degree in 1998 at the Digital Image Processing Group of the University of Cape Town. Currently he is working as a Signal/Systems Analysis Engineer on projects related mostly to Radar and RF Electronic Warfare at the CSIR, Defencetek.



Areas of interest include signal and image processing, pattern recognition, AI, machine learning and computer graphics.

Co-Author: Jan Tait holds a B.Eng. degree and M.Sc. degree in Electrical and Electronic Engineering from the University of Stellenbosch, South Africa. At present he is an engineer at the CSIR where he is involved in the development and analysis of radar and other electronic warfare systems. He has a wide field of interest, which includes analog electronics (acoustic engineering), antenna systems, RF and microwave systems and techniques, and digital signal processing.



Co-Author: R.T. Lord received a BSc degree in Electrical Engineering at the University of Cape Town, South Africa, in 1994. In 2000 he received a PhD degree at the same university, working on processing aspects of low-frequency SAR systems. He is currently doing a post-doctorate at the DLR in Germany, working on a spotlight SAR processor for the future German TerraSAR-X satellite.



His interests include radar signal processing and image processing.